

Modelling Local Patterns of Child Mortality Risk. A Bayesian Spatio-Temporal Analysis.

Alejandro Lome-Hurtado (✉ alh@azc.uam.mx)

Universidad Anahuac Mexico <https://orcid.org/0000-0003-1241-4553>

Jacques Lartigue Mendoza

Universidad Anahuac Mexico

Juan C. Trujillo

University of York

Research article

Keywords: Children's health, Bayesian mapping, child mortality risk, space-time interactions, Mexico

Posted Date: May 18th, 2020

DOI: <https://doi.org/10.21203/rs.2.11961/v3>

License: © ⓘ This work is licensed under a Creative Commons Attribution 4.0 International License.

[Read Full License](#)

Version of Record: A version of this preprint was published at BMC Public Health on January 6th, 2021.
See the published version at <https://doi.org/10.1186/s12889-020-10016-9>.

Abstract

Background: Globally, child mortality rate is still high; however, this figure is susceptible to be reduced implementing proper spatially-targeted health public policies. Due to its alarming rate in comparison to North American standards, child mortality is a particular health concern in Mexico. Despite this fact, there remains a dearth of studies that address its spatio-temporal identification in the country. The aims of this study are i) to model the evolution of child mortality risk at the municipality level in Greater Mexico City, (ii) to identify municipalities with high, medium, and low risk over time, and (iii) using municipality trends, to ascertain potential high-risk municipalities.

Methods: In order to control for the space-time patterns of data, the study performs a Bayesian spatio-temporal analysis. This methodology permits the modelling of the geographical variation of child mortality risk across municipalities, within the studied time span.

Results: The analysis shows that most of the high-risk municipalities were in the east, along with a few in the north and west areas of Greater Mexico City. In some of them, it is possible to distinguish an increasing trend in child mortality risk. The outcomes highlight municipalities currently presenting a medium risk but liable to become high risk, given their trend, after the studied period. Finally, the likelihood of child mortality risk illustrates an overall decreasing tendency throughout the 7-year studied period.

Conclusions: The identification of high-risk municipalities and risk trends may provide a useful input for policy-makers seeking to reduce the incidence of child mortality. The results provide evidence that support the use of geographical targeting in policy interventions.

Introduction

There is a public concern regarding the high percentage of child mortality. Globally, there were 5.6 million child deaths during 2016 [1]. As a consequence, an increasing policy interest in improving children's health has been witnessed, reflected in the United Nations' third Sustainable Development Goal (SDSDG) on good health and wellbeing; particularly, in its aim to end preventable deaths of new-born and children under five by the year 2030 [2][2].

Between 2010 and 2017, under-five mortality rate (per 1,000 live births) decreased from 17.4 to 13.4 in Mexico. However, these numbers are still higher than those observed in North America and other developed countries. For instance, these rates diminished, during the referenced years, from 7.3 to 6.6 in the United States, and from 5.6 to 5.1 in Canada [3][3]. Similarly, the probabilities of dying at age 5-14 years (per 1,000 children age 5) in Mexico were 2.8 in 2010 and 2.5 in 2018, while in the United States these figures were 1.3 for both years, and in Canada 1.1 and 1.0 [4][4]. By the same token, according to the World Bank [5], the Mexican infant mortality rate (per 1,000 live births) observed a reduction from 2010 to 2017, passing from 14.9 to 11.6. Nevertheless, such rates are still high in comparison to the

United States and Canada, where the figures declined, during the aforesaid years, from 6.2 to 5.7, and from 4.9 to 4.4, respectively.

This paper focuses on the modelling of child mortality risk trends across different geographical areas, with the purpose of contributing with the increasing international interest in modelling the spatial structure of such problem [6]–[9]. Within this line of research, Gayawan et al. [6] [6] illustrated the regional variations of child mortality among ten West African countries, finding some clusters of higher child mortality in northwest and northeast Nigeria. In the same line of thought, Jimenez-Soto et al. [7][7] showed the disparities among child mortality across rural-urban locations and regions in Cambodia, and analogous findings, additionally including variations within inter and inintra regions, were made in Papua, New Guinea [8][8]. In Mexico, a similar study [10] analyzed the child mortality trend caused by diarrhea in all Mexican states, identifying different spatial patterns of the peak mortality rate across time.

The relevance of coconsidering the potential spatial structure of the data is grounded on the fact that communities are often clustered with respect to certain shared characteristics, as their socioeconomic background [11][11]. Presumably, people with a high socioeconomic status live close to each other, and likewise among other socioeconomic standings. However, socioeconomic status is not the sole factor underlying child mortality; if the availability of data allows it, other variables, such as environment, urbanization, or the genetics of people, must be regarded in a spatial analysis [12], [13], [14]. McDonald et al. [13], analyzing American counties located in the US-Mexican border, found urbanization level as the most relevant variable for explaining child mortality, while ethnicity –hispanic or non-hispanic white– appeared to be less relevant. Thus, higher mortality rates in non-metropolitan communities were attributed to a diminished access to emergency and special care facilities, limited emergency medical service capabilities, as well as less health care providers per capita. Castro-Ríos et al. [14] found that access to social security increases the surviving probability of children with acute lymphoblastic leukemia. More accurately, the research concluded that children who had been insured for less than half of their lives had more than a twofold risk of death than children insured throughout their entire lives.

Child mortality may not only vary over space, but also over time, as it has been determined in previous health studies; such is the case of the spatio-temporal variations of stomach cancer risk [15] and asthma risk [16]. Besides, people's health risk may vary over space and time due to changes in health-related behaviours, namely physical activity, smoking, and diet [17]. Thus, in order to gain a better understanding, the need for analyzing not just the spatial pattern of the mortality risk but also its local trend over time, at the geographical level, becomes evident.

Therefore, this study uses a Bayesian modelling approach [18] owing to the space, time, and space-time structure of the data, while the methodology is based on random effects, which enables the modelling of the geographical variation of children mortality over time. It must be acknowledged that this methodology has been used in the area of criminology [19]. The aims of this study are (i) to model the evolution of child mortality risk at the municipality level in Greater Mexico City, (ii) to identify municipalities with high, medium, and low risk over time, and (iii) using local trends, to ascertain potential high-risk municipalities.

Data And Methods

2.1 Area of study and Child mortality data

Greater Mexico City, one of the most populated urban areas in the world, is the third largest metropolis among the OECD countries, and the world's largest outside of Asia [20]. It consists of 16 municipalities within Mexico City and 59 in the State of Mexico [1] (see figure A1 in the Appendix). According to the Mexican National Institute of Statistics and Geography (INEGI) [21], in 2015 it had 20,892,724 inhabitants, covering a land area of 7,866 square kilometers. In economic terms, it is considered the most important metropolitan area in Mexico, accounting for 23% of the country's gross domestic product in 2010 [20]. The present study explored the catalogs of death and birth records, issued by the Mexican Ministry of Health [2], of 75 municipalities within Greater Mexico City in a period spanning from January 2011 to December 2017. During this study period, the total number of live births in the region was 2,121,601, while the number of deaths of children totalled 35,862; children were considered from 0 to 5 years old [22][22]. This information was aggregated in order to perform a spatial and temporal analysis at the municipality level [23].

2.2 Statistical analysis

Preliminary analyses were carried out to investigate the potential presence of spatial autocorrelation and serial correlation of the data using the Global Moran Index [24][24] and the Autocorrelation Function (ACF). Furthermore, a Bayesian spatio-temporal model was used to model the potential spatial and temporal child mortality risk. Assuming the child mortality risk, in the municipality i , at a given period t ($t=2011, 2013, \dots, 2017$) follows a binomial distribution [25], Y_{it} . Where n_{it} represents the total number of live births in the municipality i at period t ; and d_{it} denotes the number of child deaths in the municipality i at period t . According to Law et al. [26] and Li et al. [19] child mortality risk can be modelled as:

[Please see the supplementary files section to view the equation.] (1)

where α is the overall logit child mortality risk across the 7-year period and the terms μ_i and ν_t are the spatial components, which capture the spatial structure and unstructured effects of the data respectively. These components are common among the study period. Additionally, β is the overall time trend in all of the municipalities. The first term (βt) assesses the linear trend, and the second (βt^2) , with additional Gaussian noise, allows for nonlinearity in the overall trend pattern; follows a normal distribution, ϵ_{it} . Note that β is centered at the mid observation period, $t = 4$. The expression βt^2 denotes the spatio-temporal structure of the data, which permits each municipality to have a different trend from the overall time trend-pattern. This

term plays an important role considering that child mortality trends exhibit variability at the local level (see figure 1). Thus, μ_i represents, and assumes, a linear departure of the municipality temporal trend from the common trend; such local trend can have an increasing, decreasing or stable tendency from the overall linear pattern. Finally, σ_i is the component addressed to contain the variability that is not explained by other terms, and may include overdispersion; that is, when the variation of the data is higher than its mean – a common characteristic of binomial models [27], [28].

We assigned the BYM (Besag, York, and Mollié) model [29] to the spatial components μ_i . Following previous studies [18], [19], [25] we allocated an intrinsic conditional autoregressive Gaussian distribution (ICAR) to the priors of the spatial structure (μ_i) and to the spatio-temporal interaction term (σ_i) . Thus, the terms μ_i and σ_i depend on the neighbouring, meaning that near areas are more likely to have similar values; in our specific case, it means that nearby municipalities are assumed to have similar child mortality risk rates. This is controlled by a spatial adjacency matrix W of size $N \times N$, where the diagonal values are $w_{ii}=0$ and the off-diagonal entries $w_{ij}=1$ if municipalities i and j share a common boundary, otherwise $w_{ij}=0$. In this sense, if two municipalities are defined to be neighbours their random effects are correlated, otherwise they are conditionally independent. The conditional expectation of μ_i is equal to the mean of the random effects in neighbouring municipalities, whereas the conditional variance is inversely proportional to the number of neighbour municipalities, this is similar for σ_i . Note that σ_i may also control for the potential endogeneity due to the interaction between space and time. In accordance to previous studies' proceedings, [19], [25] we allocated an hyperprior distribution of Gamma, a highly non-informative distribution [30][30], on the variance of μ_i and σ_i . We assigned a Gaussian distribution to the spatially unstructured random effect term, η_i . Finally, following the Gelman criterion [31], all random effect standard deviations, such as σ_i and η_i , have a positive half Gaussian prior σ_i .

To classify each municipality into hot, cold or neither-hot-nor-cold spots (high, low or medium risk) across time, we used the values of the posterior probability of the spatial component μ_i . The component μ_i indicates the odds average risk of the study period for each municipality with respect to μ (overall logit children mortality risk). Thus, the values greater than 0.8, between 0.2 and 0.8, and lower than 0.2 were classified as hot, neither-hot-nor-cold, and cold spots (high, medium, and low risk municipalities), respectively. This first classification can be expressed in the term h_i which is equal to 1 for a hot spot, 2 for a cold spot, and 3 for a neither-hot-nor-cold spot. This criterion has been used in previous studies [19], [32]. Further, to measure the local trend of each classified municipality, we used the values of the posterior probability of the local slopes β_i given a specific category of h_i . This technique enabled the measurement of each municipality's local dynamic pattern throughout the study period. Thus, if β_i , or σ_i the municipality was classified as having an increasing, decreasing or stable trend, in comparison with the overall trend.

The model was implemented in R [33][33] and WinBUGS[34] [34] (statistical software). We ran MCMC chains of 100,000 (for this number the model reaches convergence) with different initial values. 70,000 iterations were used for making inferences from the model, after having burned in the first 30,000. The convergence was examined by visual inspection of the history plots and through the Gelman-Rubin diagnostic [31], which are standard statistical tests to measure convergence of MCMC chains. The values

from the Gelman-Rubin diagnostic remained lower than 1.04 for every single model parameter, meaning that the chains achieved convergence after the burn-in period.

[1] There is one more municipality belonging to the State of Hidalgo, which is excluded from this analysis.

[2] Publicly available online at

http://www.dgis.salud.gob.mx/contenidos/basesdedatos/Datos_Abiertos_gobmx.html

Results

3.1 Descriptive Analysis

The Global Moran Index of the data for each year was positive and significant, with a mean value of 0.32 and a p value < 0.0001 , illustrating the presence of a positive spatial correlation in the records. In other words, this result is indicative of the existence of some nearby municipalities with a similar mortality risk. The ACF mean was 0.58 (lagged 1 year for each municipality) across all the municipalities. This number evidences the presence of serial correlation; that is, the association of certain level of observed mortality across time.

Table 1 provides a descriptive statistics overview of the observed child mortality rate in Greater Mexico City from 2011 to 2017, defined as the number of deaths of children aged 0 to 5 years, per 1,000 live births. Broadly, there was a slight mitigation on the average child mortality rate during these years, shifting from 20.4 in 2011 to 17.47 in 2017. Note that according to the means and variances, illustrated in table 1, a trace of overdispersion was present in our data.

Insert Table 1

Figure 1 depicts the temporal evolution of the observed child mortality risk by municipality in Greater Mexico City, at different years –2011, 2014, and 2017 (start, middle, and end)– throughout the study period. The dark green and red colors indicate the lowest and highest risks, respectively. Overall, municipalities with higher risk were enclosed in the east, besides a few scattered in the north. Conversely, municipalities with the lowest mortality risk clearly constituted a cluster in the south-west (stronger green color).

Insert Figure 1

3.2 Modelling spatial-temporal patterns

Figure 2a illustrates the odds of child mortality risk by municipality, compared to the average throughout the studied period. An odd risk value above or below 1 suggests a higher or lower risk associated with the concerning municipality, in comparison to the Greater Mexico City 7-year average. The figures mainly display that municipalities menaced by a higher child mortality risk are those situated in the surroundings of Mexico City: the east area, along with a few in the north. Concurrently, municipalities located in Mexico City, as well as a few in the north of the studied area, presented lower risks. Figure 2b illustrates the overall time trend of the relative risk in comparison to the Greater Mexico City average from 2011 to 2017. It is possible to observe, overall, a slight decreasing tendency of such risk.

Insert Figures 2a and 2b

Figures 3a, 3b, and 3c display hot spots (high risk), neither-hot-nor-cold spots (medium risk), and cold spots (low risk) of child mortality risk by municipality. Of the total, high risk municipalities amounted to 27 (36%), medium risk to 29 (39%), and low risk to 19 (25%). On the whole, high risk municipalities were located in the east of the metropolitan area along with a few spots in the north and west (see Figure 3a). Meanwhile, most of the low risk municipalities were located in the south-west (figure 3c). Finally, medium risk municipalities, on the other hand, were mostly situated in the north, in addition to a few of them scattered in the east, center, and west, as figure 3b exhibits. All of these classified municipalities were significant at the 95% Credible Interval (CI).

The inserted small graphs in figures 3a, 3b, and 3c show the different trends of the observed risk (black solid dots), the estimated risk (dashed line with open circles) with 95% CI (grey region), and the estimated common trend (black line) of the mortality risk over time.

Insert Figure 3a

Figure 3a exhibits that most of the high-risk municipalities (74%) had a stable dynamic regarding their child mortality risk trend, whereas in 4 of them (15%) showed to be increasing. The remaining 3 high-risk municipalities (11%) were the only ones with a decreasing trend over time. Figure 3b depicts medium risk municipalities, 24% of which exhibited an increasing trend in risk. The majority of the medium risk municipalities (62%) presented a stable tendency, whereas municipalities with a decreasing trend amounted to 14%.

Insert Figure 3b

Finally, Figure 3c illustrates that 21% of low risk municipalities experienced a relative increment in child mortality risk over time. However, most of these low risk municipalities (63%) had a stable trend during the studied period, leaving just 16% of municipalities under the category of decreasing trend.

Insert Figure 3c

Discussion

This research studied child mortality dynamics across municipalities in Greater Mexico City. It identified municipalities with high child mortality risk, as well as those with medium risk that, given their trend, may become high risk.

Our findings illustrate that 36% of the total municipalities fit into a high-risk categorization. These municipalities are, overall, located in the east of Greater Mexico City, along with a few spots in the north and west. This is an expected result given that Mexico City (see figure A1 in the Appendix) holds the best economic and socioeconomic conditions, while the surrounding municipalities have lower economic and social standings. According to INEGI, the north, west, and east areas of Greater Mexico City are characterized by their relatively lower socioeconomic and education levels with respect to the average (see figure A2 in the Appendix). The previous results are in line with SSreeramareddy C. et al. [35][35], and Aheto J. [36][36], who identify a positive association between deprived economic conditions and child mortality risk; the lower the level of income, the greater the probabilities of higher child mortality rates.

In terms of risk evolution, four high-risk municipalities (Chalco, Chicoloapan, Texcoco and Tonanitla), mostly located in the west, exhibited an increasing trend over time. Similarly, seven medium risk municipalities (Miguel Hidalgo, Chiconcuac, Nextlalpan, Ozumba, Teoloyucan, Tequixquiac and Tultepec), accounting for 24% of the total in that category, manifested an increasing trend over time, representing their liability to become high risk in the short term. Six of these seven municipalities are in the north area. As figure A2 in the Appendix depicts, these municipalities with high and medium risk face deprived economic and social conditions, with the exception of Miguel Hidalgo. These results are congruent with those of Escamilla-Santiago et al. [37][37], who evidenced, for the period between 1990 - 2009, an increasing cancer mortality rate in children and teenagers residing in high marginalized Mexican states.

It must be acknowledged that a decreasing trend manifested in the average mortality risk likelihood over the 7-years studied period. This result coincides with Aguirre A. and Vela-Peóns work [38][38], who estimated, by deploying the Brass mortality method, a decreasing infant mortality rate in Mexico from

1990 to 2010. This slight decrement may partially be explained as the result of diverse public health policies, such as the public programs aimed at decreasing neonatal mortality risk, deployed by the Mexican Ministry of Health. These include “Programa de Acción: Arranque Parejo en la Vida, 2002”, “Programa de Acción Específico 2007-2012, 2008” and “Programa de Acción Específico Salud Maternal y Perinatal, 2013-2018” [39].

Finally, it should be acknowledged that, owing to data limitations, the results here exposed require a word of caution. Specifically, we assumed no mobility of children. Although this assumption may not apply in a dynamic area such as Greater Mexico City, more precise unavailable data would be required to permit the consideration of this factor. Consequently, as in other studies [40], [41], the mobility of people was not included. Despite the previous constraint, we hope the key strengths of this study, including space, time, and space-time structures, may provide relevant insights for diminishing child mortality risk in Greater Mexico City. In this sense, McLaughlin et al. [42] highlight the importance of spatial data and the local context, as inputs for policy decisions. Likewise, in the area of health, Ugarte et al. [36][36] illustrate how spatial and temporal trends provide useful information for addressing health inequalities. However, in order to complement this study, future studies should aim to investigate additional potential factors underlying the mortality of children.

Conclusion

By unearthing the identification and evolution of child mortality risk on municipalities belonging to Greater Mexico City, the findings of this research may provide an important input for policy decisions addressed to reduce the mortality of children. Locations with high child mortality risk should be benefited from priority interventions. In this sense, this analysis provides important baseline information for decision-makers. The identification of spatial and temporal trends across different areas supplies decision-makers with relevant inputs for designing programs to tackle health inequalities [44][44]. Using these inputs, spatially targeted programs may focus on small locations, allowing policy measures to have a more effective local impact. In this regard, it has already been demonstrated that in comparison with programs where resources are not addressed towards specific geographical areas [45], [46], vulnerable and local groups benefit more when the aforementioned inputs are used. This study identified municipalities with medium and high child mortality risk, especially those with an increasing trend over time (Chalco, Chicoloapan, Texcoco and Tonanitla, in the case of high child mortality risk), which helps to implement the geographical targeting of policy efforts to reduce it. Given the overall scarcity of healthcare resources in Mexico, we hope these results may contribute to the improvement of cost-effective policies.

Declarations

Ethics approval and consent to participate

Not applicable

Consent for publication

Not applicable

Availability of data and material

Data are freely available at:

http://www.dgis.salud.gob.mx/contenidos/basesdedatos/Datos_Abiertos_gobmx.html

Competing interests

The authors declare that they have no competing interests.

Funding

No funding required

Authors' contributions

ALH developed the spatio-temporal statistical model and performed the model programming, fitting and interpretation of the results. He drafted the sections in this paper.

All the authors contributed to the design of the study.

JCT and JLM contributed with the introduction, discussion, and conclusions. They wrote the final manuscript.

All authors read and approved the final manuscript.

Acknowledgements

We are grateful with Li Guanquan for the meetings with ALH which favoured the properly understanding of the Bayesian model; as well as with Paloma Botello, Mekuria Asfaw and Oyelola A. Adegboye for their enlightening comments / feedback that helped in the improvement of this paper.

References

[1] You D., Hug L., Ejdemyr S., Idele P., Hogan D., Mathers C., Gerland P., New J.R., Alkema L. Global, regional, and national levels and trends in under-5 mortality between 1990 and 2015, with scenario-based projections to 2030: A systematic analysis by the UN Inter-agency Group for Child Mortality Estimation. *The Lancet*. 2015 Dec 5;386(10010):2275-86.

- [2] Nations, U., "Sustainable development goals," (*n.d.*). [Online]. Available: <https://www.un.org/sustainabledevelopment/health>. Accessed 3 June 2019.
- [3] Bank, T. W., "Mortality rate, under-5 (per 1,000 live births)," (*n.d.*). [Online]. Available: <https://data.worldbank.org/indicator/SH.DYN.MORT?end=2017&locations=MX&start=1960&view=chart>. Accessed 3 June 2019.
- [4] Hill K., Zimmerman L., Jamison D.T. Mortality risks in children aged 5–14 years in low-income and middle-income countries: A systematic empirical analysis. *The Lancet Global Health*. 2015 Oct 1; 3(10):e609-16.
- [5] Bank, T. W., "Mortality rate, infant (per 1,000 live births)," (*n.d.*). [Online]. Available: <https://data.worldbank.org/indicator/SP.DYN.IMRT.IN?view=chart>. Accessed 3 June 2019.
- [6] Gayawan E., Adarabioyo M.I., Okewole D.M., Fashoto S.G., Ukaegbu J.C. Geographical variations in infant and child mortality in West Africa: A geo-additive discrete-time survival modelling. *Genus*. 2016 Dec; 72(1):5.
- [7] Jimenez-Soto E., Durham J., Hodge A. Entrenched geographical and socioeconomic disparities in child mortality: Trends in absolute and relative inequalities in Cambodia. *PloS one*. 2014; 9(10).
- [8] Bauze A.E., Tran L.N., Nguyen K.H., Firth S., Jimenez-Soto E., Dwyer-Lindgren L., Hodge A, Lopez A.D. Equity and geography: The case of child mortality in Papua New Guinea. *PLoS One*. 2012; 7(5).
- [9] Singh A., Pathak P.K., Chauhan R.K., Pan W. Infant and child mortality in India in the last two decades: A geospatial analysis. *PLoS One*. 2011; 6(11).
- [10] Alonso, A. W. J. *et al.* Spatio-temporal patterns of diarrhoeal mortality in Mexico," 2019; 140(1); 91–99.
- [11] Knorr-Held L., Besag J. Modelling risk from a disease in time and space. *Statistics in Medicine*. 1998 Sep 30; 17(18):2045-60.
- [12] Lome-Hurtado A., Touza-Montero J., White P.C. Environmental Injustice in Mexico City: A Spatial Quantile Approach. *Exposure and Health*. 2019:1-5.
- [13] McDonald J.A., Brantley L., Paulozzi L.J. Mortality, Ethnicity, and Urbanization Among Children Aged 1-4 Years on the US-Mexico Border. *Public Health Reports*. 2018 Sep; 133(5):593-600.
- [14] Castro-Ríos A., Reyes-Morales H, Pelcastre-Villafuerte B.E., Rendón-Macías M.E., Fajardo-Gutiérrez A. Socioeconomic inequalities in survival of children with acute lymphoblastic leukemia insured by social security in Mexico: A study of the 2007–2009 cohorts. *International Journal for Equity in Health*. 2019 Dec 1; 18(1):40.

- [15] Papoila A.L., Riebler A., Amaral-Turkman A., São-João R., Ribeiro C., Geraldés C., Miranda A. Stomach cancer incidence in Southern Portugal 1998–2006: A spatio-temporal analysis. *Biometrical Journal*. 2014 May; 56(3):403-15.
- [16] Lawson A.B. *Bayesian disease mapping: Hierarchical modeling in spatial epidemiology*. CRC press; 2013 Mar 18.
- [17] Shin H.H., Stieb D., Burnett R., Takahara G., Jessiman B. Tracking national and regional spatial-temporal mortality risk associated with NO₂ concentrations in Canada: A Bayesian hierarchical two-level model. *Risk Analysis: An International Journal*. 2012 Mar; 32(3):513-30.
- [18] Bernardinelli L., Clayton D., Pascutto C., Montomoli C., Ghislandi M., Songini M. Bayesian analysis of space–time variation in disease risk. *Statistics in Medicine*. 1995 Nov 15;14(21-22):2433-43.
- [19] Li G, Haining R., Richardson S., Best N. Space–time variability in burglary risk: A Bayesian spatio-temporal modelling approach. *Spatial Statistics*. 2014 Aug 1;9:180-91.
- [20] (OECD), O. for E. C. and D., “Territorial Reviews: Valle de México, Mexico,” 2015. [Online]. Available: http://www.keepeek.com/Digital-Asset-Management/oecd/urban-rural-and-regional-development/oecd-territorial-reviews-valle-de-mexico-mexico/urban-trends-and-challenges-of-the-valle-de-mexico_9789264245174-5-en. Accessed 3 June 2019.
- [21] (INEGI), M. N. I. of S. and G., “Población,” (*n.d.*). [Online]. Available: <https://www.inegi.org.mx/temas/estructura/>. Accessed 3 June 2019.
- [22] Administration, U. F. and D., “General clinical pharmacology considerations for pediatric studies for drugs and biological products. *Clinical Pharmacology*,” 2014. [Online]. Available: <https://www.fda.gov/Drugs/GuidanceComplianceRegulatoryInformation/Guidances/default.htm>. Accessed 3 June 2019.
- [23] Lome-Hurtado, A., “Child mortality data set in Greater Mexico City,” *Mendeley Data*, vol. 1, 2019.
- [24] Anselin L., Bera A.K., Florax R., Yoon M.J. Simple diagnostic tests for spatial dependence. *Regional Science and Urban Economics*. 1996 Feb 1;26(1):77-104.
- [25] McCullagh, P., *Generalized linear models*. Routledge, 2019.
- [26] Law J., Quick M., Chan P. Bayesian spatio-temporal modeling for analysing local patterns of crime over time at the small-area level. *Journal of Quantitative Criminology*. 2014 Mar 1; 30(1):57-78.
- [27] Dean C.B. Testing for overdispersion in Poisson and binomial regression models. *Journal of the American Statistical Association*. 1992 Jun 1; 87(418):451-7.

- [28] Yang Z, Hardin J.W., Addy C.L. A note on Dean's overdispersion test. *Journal of Statistical Planning and Inference*. 2009 Oct 1; 139(10):3675-8.
- [29] Besag, J., J. York, and A. Mollié, "A Bayesian image restoration with two applications in spatial statistics *Ann Inst Statist Math* 43: 1–59," *Find this Artic. online*, vol. 43, no. 1, pp. 1–20, 1991.
- [30] Kelsall, J. E. and J. C. Wakefield, "Discussion of 'Bayesian models for spatially correlated disease and exposure data', by Best et al," *Bayesian Stat.*, vol. 6, p. 151, 1999.
- [31] Gelman A., Rubin D.B. Inference from iterative simulation using multiple sequences. *Statistical Science*. 1992; 7(4):457-72.
- [32] Richardson S., Thomson A., Best N, Elliott P. Interpreting posterior relative risk estimates in disease-mapping studies. *Environmental Health Perspectives*. 2004 Jun; 112(9):1016-25.
- [33] R Core Team (2013), "R: A language and environment for statistical computing. R Foundation for Statistical Computing, Vienna, Austria". Accessed 3 June 2019.
- [34] Lunn D.J., Thomas A., Best N., Spiegelhalter D. WinBUGS-a Bayesian modelling framework: Concepts, structure, and extensibility. *Statistics and Computing*. 2000 Oct 1; 10(4):325-37.
- [35] Sreeramareddy C.T., Kumar H.H, Sathian B. Time trends and inequalities of under-five mortality in Nepal: A secondary data analysis of four demographic and health surveys between 1996 and 2011. *Plos One*. 2013; 8(11).
- [36] Aheto J.M. Predictive model and determinants of under-five child mortality: Evidence from the 2014 Ghana demographic and health survey. *BMC Public Health*. 2019 Dec 1; 19(1):64.
- [37] Escamilla-Santiago R.A., Narro-Robles J., Fajardo-Gutiérrez A., Rascón-Pacheco R.A., López-Cervantes M. Tendencia de la mortalidad por cáncer en niños y adolescentes según grado de marginación en México (1990-2009). *Salud Pública de México*. 2012;54(6):587-94.
- [38] Aguirre A., Vela-Peón F. La mortalidad infantil en México, 2010. *Papeles de Población*. 2012 Sep; 18(73):29-44.
- [39] Mexico, M. of H. in, "Program de Accion Especifico. Salud Maternal y Perinatal," 2014. [Online]. Available: <https://www.gob.mx/cms/uploads/attachment/file/242370>. Accessed 3 June 2019.
- [40] Havard S., Deguen S., Zmirou-Navier D., Schillinger C., Bard D. Traffic-related air pollution and socioeconomic status: A spatial autocorrelation study to assess environmental equity on a small-area scale. *Epidemiology*. 2009 Mar 1:223-30.
- [41] Fecht D., Fischer P., Fortunato L., Hoek G., de Hoogh K., Marra M., Kruize H., Vienneau D., Beelen R., Hansell A. Associations between air pollution and socioeconomic characteristics, ethnicity and age profile

of neighbourhoods in England and the Netherlands. *Environmental Pollution*. 2015 Mar 1; 198:201-10.

[42] McLaughlin L.M., Johnson S.D., Bowers K.J., Birks D.J., Pease K. Police perceptions of the long- and short-term spatial distribution of residential burglary. *International Journal of Police Science & Management*. 2007 Jun; 9(2):99-111.

[43] Aragonés N., Goicoa T., Pollán M., Militino A.F., Pérez-Gómez B., López-Abente G., Ugarte M.D. Spatio-temporal trends in gastric cancer mortality in Spain: 1975–2008. *Cancer Epidemiology*. 2013 Aug 1;37(4):360-9.

[44] Ugarte M.D., Adin A., Goicoa T., Casado I., Ardanaz E., Larrañaga N. Temporal evolution of brain cancer incidence in the municipalities of Navarre and the Basque Country, Spain. *BMC Public Health*. 2015 Dec;15(1):1018.

[45] Smith G. Area-based initiatives: The rationale and options for area targeting. LSE STICERD Research Paper No. Case025. 1999 May.

[46] Tunstall, R. and R. Lupton, “Is Targeting Deprived Areas an Effective Means to Reach Poor People? An assessment of one rationale for area-based funding programmes,” 2003.

Table

Table 1. Descriptive statistics. Observed child mortality rate¹ in Greater Mexico City (2011 to 2017)

Observed child mortality risk	2011 year	2012 year	2013 year	2014 year	2015 year	2016 year	2017 year
Mean	20.4	19.91	18.42	18.12	18.97	17.08	17.47
Standard deviation	8.18	7.03	6.09	6.39	8.87	7.41	5.26
Minimum value ²	1.92	1.49	2.16	2.32	2.22	1.74	3.3
Maximum value ³	58.39	51.02	35.64	34.3	60.34	55.56	35.71

1/ Child mortality rate = (child deaths / number of resident live births) x 1000. In other words, number of child deaths per 1,000 resident live births.

2/ Corresponds to the municipality with the minimum value among all the municipalities of Greater Mexico City.

3/ Corresponds to the municipality with the maximum value among all the municipalities of Greater Mexico City.

Figures

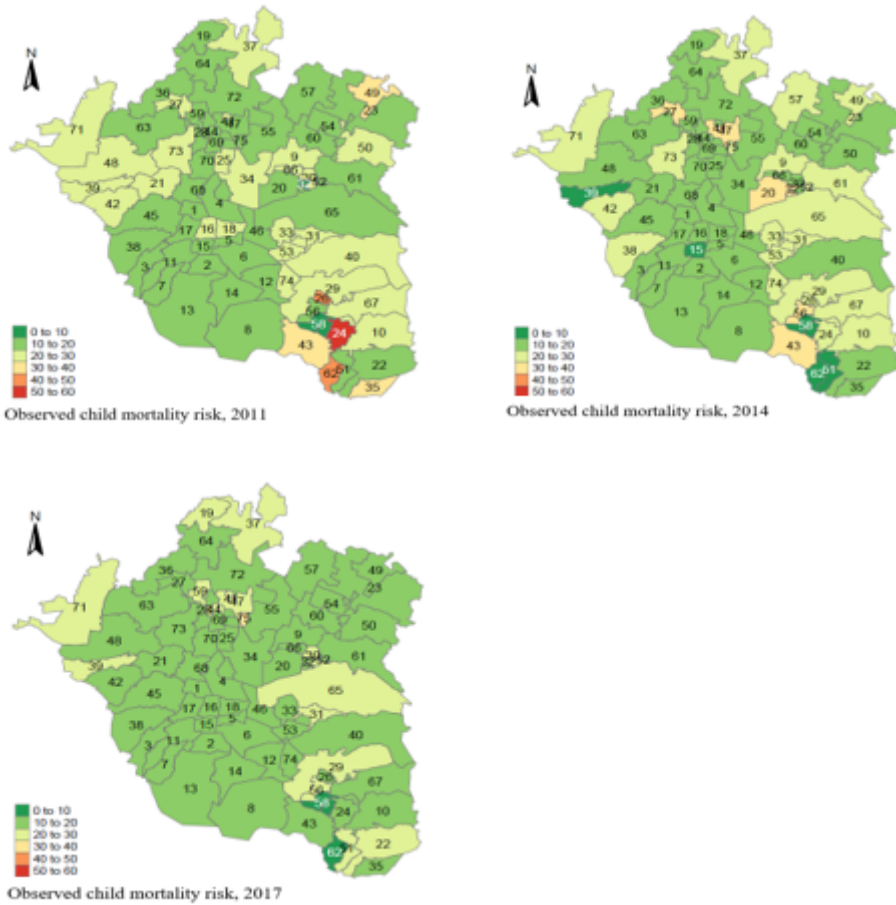


Figure 1

Geographical pattern evolution of the observed child mortality risk (per 1,000 live births) in Greater Mexico City. Figure 1 depicts the temporal evolution of the geographical pattern of the observed child mortality risk (per 1,000 live births) in Greater Mexico City, at the start (2011), middle (2014), and end (2017) of the studied period. Source: Own elaboration using data from INEGI and Mexican Ministry of Health.

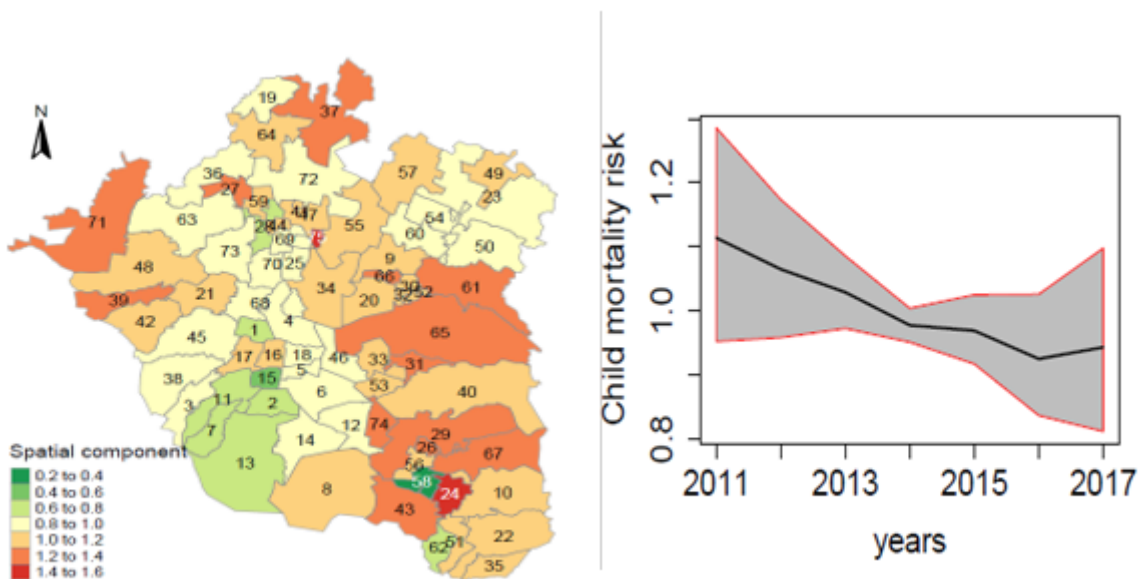


Figure 2

Spatial child mortality odd risk at the municipality level and overall trend in Greater Mexico City. Figure 2a shows the spatial component of child mortality odd risk during the studied period. Areas with odd risk values greater or lower than 1, have higher or lower odd risks in comparison with the average, respectively. Figure 2b displays the overall odd risk trend, with a 95% CI, from 2011 to 2017. Source: Own elaboration using data from INEGI and Mexican Ministry of Health.

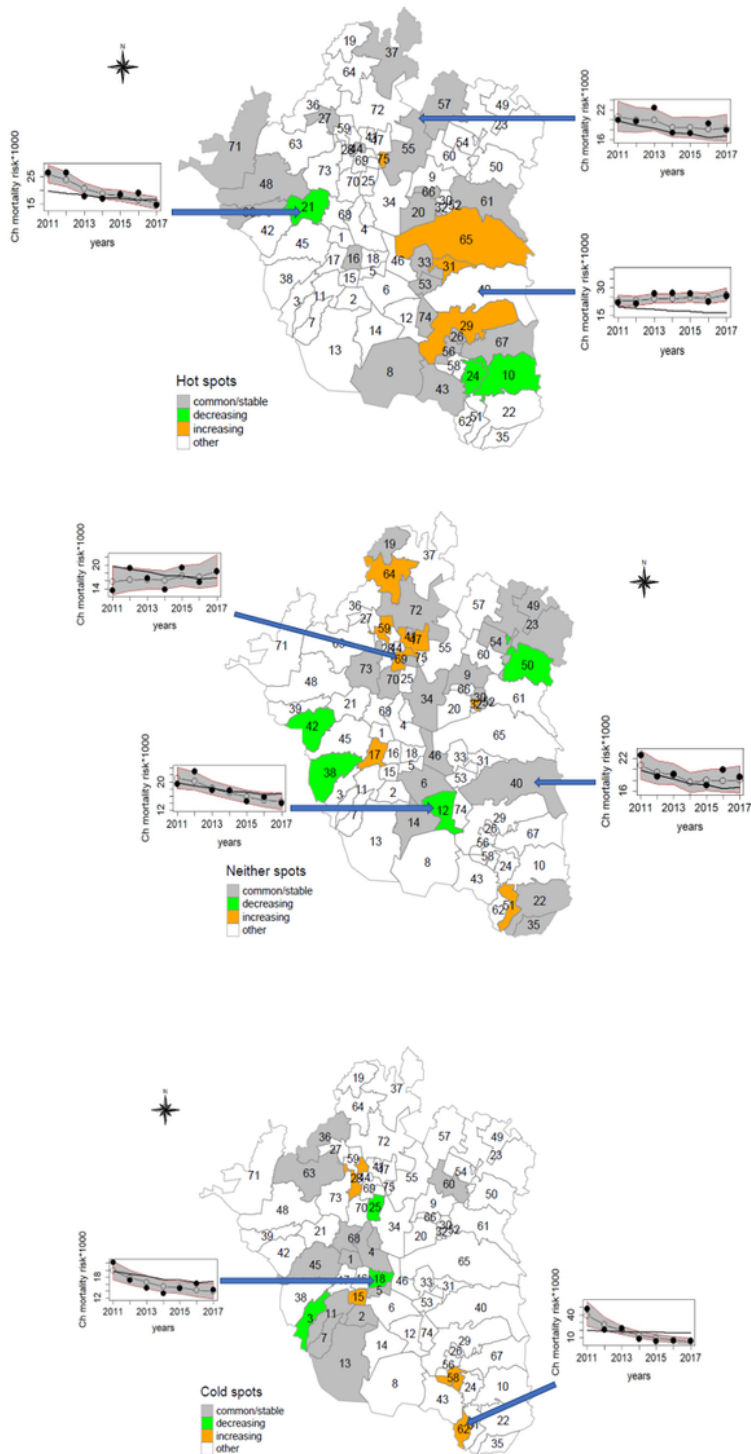


Figure 3

Figure 3a. Temporal trend in child mortality risk for high-risk municipalities Figure 3a displays the temporal dynamics of child mortality risk for high-risk municipalities in Greater Mexico City, which are classified into 3 categories: stable, decreasing and increasing risk. The inserted figures show the observed child mortality risk (black solid dots), the estimated child mortality risks –posterior means of risks– (open circles and dashed line) with a 95% CI (grey region) and the estimated common trend (black line) over time. Source: Own elaboration using data from INEGI and Mexican Ministry of Health. Figure 3b. Temporal trend in child mortality risk for medium-risk municipalities Figure 3b displays the temporal dynamics of child mortality risk for medium-risk municipalities in Greater Mexico City, which are classified into 3 categories: stable, decreasing and increasing risk. The inserted figures show the observed child mortality risk (black solid dots), the estimated child mortality risks –posterior means of risks– (open circles and dashed line) with a 95% CI (grey region) and the estimated common trend (black line) over time. Source: Own elaboration using data from INEGI and Mexican Ministry of Health. Figure 3c. Temporal trend in child mortality risk for low-risk municipalities Figure 3c displays the temporal dynamics of child mortality risk for low-risk municipalities in Greater Mexico City, which are classified into 3 categories: stable, decreasing and increasing risk. The inserted figures show the observed child mortality risk (black solid dots), the estimated child mortality risks –posterior means of risks– (open circles and dashed line) with a 95% CI (grey region) and the estimated common trend (black line) over time. Source: Own elaboration using data from INEGI and Mexican Ministry of Health.

Supplementary Files

This is a list of supplementary files associated with this preprint. Click to download.

- [Equation.docx](#)
- [LomeHurtadoetalAppendixamendedMAY.docx](#)